

The Sleuth Transit Survey: Understanding the Formation, Physical Structure and Atmospheric Composition of Hot Jupiters

Francis T. O'Donovan*

California Institute of Technology

ABSTRACT

The discovery of new transiting gas giants and the detailed study of these planets provide crucial constraints on their atmospheric and internal structures and on how gas giants are formed. I propose as the major component of my thesis research to continue the Sleuth campaign as part of the Trans-atlantic Exoplanet Survey (TrES) survey for extrasolar transiting planets. I will also perform followup photometry with Sherlock on the candidates that result from this survey, concurrent with TrES multiepoch spectroscopy of these objects, and will employ both sets of observations to eliminate false positives. I will use facilities such as the Keck Observatory, Hubble Space Telescope and Spitzer Space Telescope to conduct detailed followup studies of the objects detected by TrES.

1. The Nature of Planets Beyond the Solar System

Prior to the discovery of the first extrasolar gas giant (51 Peg b: Mayor & Queloz 1995), models of the formation and evolution of planetary systems were based solely on our solar system. Approximately 134 planetary systems with 152 extrasolar gas giants¹ around main-sequence stars are now known, providing a wealth of new data. Most extrasolar planets have been identified from Doppler surveys, which search for the radial velocity variation of a star caused by the presence of a massive gas giant. From the amplitude (A), period (P) and shape of this variation, the semi-major axis (a) and eccentricity (e) of the planet's orbit

*Advisor: Prof. David Charbonneau, Harvard University.

Local Advisor: Prof. Lynne Hillenbrand, California Institute of Technology.

¹Up-to-date figures available from the Extra-solar Planets Catalog:
<http://cfa-www.harvard.edu/planets/catalog.html>.

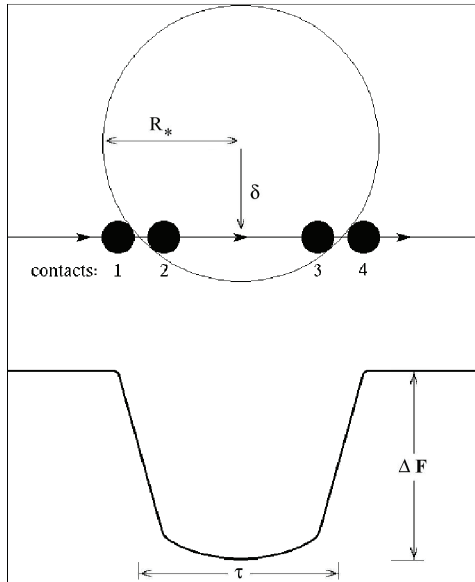


Fig. 1.— The light curve of a star (radius R_*) as an object transits at a stellar latitude δ . (Adapted from Brown et al. 2001.) The light curve shows an ingress (contacts 1–2), a fairly flat transit (2–3) and an egress (3–4). The deviation from a flat transit is caused by stellar limb darkening. There is an overall decrease in brightness of ΔF and τ is the transit duration.

can be calculated, together with its minimum mass ($m \sin i$, where m is the actual mass of the planet and i is the orbital inclination). The diverse range in values for these parameters has drastically altered our theoretical appreciation of the development of planetary systems. For example, it was realized that gas giants could be found much closer to their parent stars and have shorter orbital periods than is the case in the solar system. Jupiter completes an orbit in 12 years, while of the currently known extrasolar Jupiter–mass objects, 20% (~ 32) have orbital periods of less than 10 days. These extrasolar planets, called “hot Jupiters”, are highly irradiated by their stars which lie within 0.1 AU. (For comparison, Mercury orbits the Sun at 0.387AU.)

The proximity of a hot Jupiter to the star increases the likelihood that we can observe the planet passing in front of the stellar disk (of radius R_*). This probability for a hot Jupiter orbiting a solar–type star is given by $p \sim R_*/a \sim 10\%$. If a transit does occur, the occultation by the planetary disk of radius r causes a periodic dimming of the starlight, given by $\Delta F = (r/R_*)^2$. Hence, a Jupiter occulting a solar–type star will cause a $\sim 1\%$ dip in brightness. Figure 1 illustrates the shape of the light curve from the system.

Although transits of Venus and Mercury across the Sun have been recorded since 1631,

it was not until much more recently that the idea emerged that extrasolar planets could be detected from transit observations (Struve 1952). Yet the large orbital distances of the solar system planets implied that transits of such objects were unlikely ($p \sim 0.01\%$ for Jupiter at 5.2 A.U.). Worse still, repeated observations over multiple orbits would be required for verification, and would take tens of years. With the discovery of hot Jupiters, it was recognized that their transits would be more likely ($p \sim 10\%$), and would occur on a timescale of days. The first successful transit detections were made by Charbonneau et al. (2000) and Henry et al. (2000). They found that the planet HD 209458 b (Mazeh et al. 2000) occults its parent star every 3.52 days, and demonstrated that it was feasible to obtain a photometric precision capable of detecting a 1% transit with photometric variability studies². Both groups were able to obtain their measurements with small-aperture telescopes: the 10 cm STARE telescope and the 0.8 m APT.

The study of HD 209458 b and the more recently discovered transiting gas giants provides a rich new source of information about these planets. Since $\sin i \sim 1$ for a transiting planet, we can obtain the true mass of the planet from the spectroscopic minimum mass. We can then derive the density and surface gravity of the planet, using the planetary radius measured from the transit light curve. Obtaining the densities and surface gravities of several planets will enable us to differentiate between current physical structure and planet formation models. There are two competing models for the formation of giant planets. Core accretion (Pollack 1984; Pollack et al. 1996) involves the slow accumulation of rock and ice into a dense core over several million years. Once this core reaches a critical mass of approximately $10M_{\oplus}$, it rapidly ($\tau \sim 10^5\text{yr}$) accretes gas from the surrounding nebula. Gravitational collapse (Boss 1997, 2000, 2001) does not require the presence of a core, and takes place on the shorter dynamical timescales ($\tau \sim 10^3\text{yr}$). Spiral instabilities in the nebular disk result in the formation of progenitor protoplanets which then collapse further to form gas giants. The two models predict different planetary radii: for a given mass, the theoretical radii of planets with cores are smaller than those formed by gravitational instability, and the smaller the mass of the planet, the larger the disagreement between the theoretical radii (Bodenheimer et al. 2003; Laughlin et al. 2005). For a close-in planet with a mass of Jupiter and heated by insolation to $T_{\text{eff}} \sim 1500\text{K}$, this difference is about $0.08R_J$, measurable using transit observations. More transiting planets must be observed and their radii calculated before we

²A survey which observes n transit events of depth d (each lasting t seconds) with a precision of σ per measurement can detect the transiting planet with a confidence of s sigma, where

$$s = \frac{d}{\sigma} \sqrt{\frac{nt}{b}}, \quad (1)$$

and b is the bin width for averaging the observations.

know which model is applicable.

Monitoring transiting planets also provides unique opportunities to determine the composition of their atmospheres. With spectroscopic observations of the primary eclipse, we can study the planetary atmospheric absorption. Charbonneau et al. (2002) detected Na absorption in the lower atmosphere of HD 209458 b, which is also thought to have a HI outflow from an extended upper atmosphere (Vidal-Madjar et al. 2003). Spectroscopy during the secondary eclipse may show thermal emission from which we can derive the temperature of the planet (Charbonneau et al. 2005).

We can probe the space surrounding transiting planets for other bodies. Brown et al. (2001) looked for satellites and rings around HD 209458 b, but found no evidence for either. Also, photometry of the secondary eclipse can determine the planet’s eccentricity. Since tidal dissipation of a non-zero eccentricity might heat the planet and expand its radius (Bodenheimer et al. 2001, 2003), knowing the eccentricity is important in understanding the mass–radius relationship for gas giants.

These motivations and the results of the transit observations of HD 209458 b have spawned numerous transit campaigns (see Horne 2003 and “Transit Search Programmes”³) with different observing techniques and target field locations. The most fruitful to date is the Optical Gravitational Lensing Experiment (OGLE–III: Udalski et al. 2002a,b,c, 2003). The authors observed 5 million stars ($I \sim 13$ –18 mag) from fields in the Galactic disk using the 1.3 m Warsaw telescope at the Las Comarcas Observatory. They performed a transit search on the light curves of a color-selected subset of approximately 150,000 stars and presented 137 candidate transiting planets. Of these, five have been confirmed: three “very hot” Jupiters with periods of around 1.5 days (OGLE–TR–56 b: Konacki et al. 2003; OGLE–TR–113 b: Konacki et al. 2004b; OGLE–TR–132 b: Bouchy et al. 2004) and two “normal” hot Jupiters with periods of 4.0 days (OGLE–TR–111 b: Pont et al. 2004) and 3.1 days (OGLE–TR–10 b: Konacki et al. 2004a).

A wide range in stellar magnitudes is being targeted for these campaigns. A deep ($I \sim 18$ –21 mag) search of stars in the Galactic plane is being performed by the EXtrasolar PLANet Occultation REsearch (EXPLORE: Mallén-Ornelas et al. 2003) project using a 4 m class telescope. On the other end of the magnitude scale is the Hungarian Automated Telescope (HAT: Bakos et al. 2002), a 65 mm telescope which monitors thousands of bright ($I \sim 6$ – 13 mag) target stars in a wide field-of-view.

Transit surveys with small aperture telescopes benefit from the brightness of the tar-

³<http://star-www.st-and.ac.uk/~kdh1/transits/table.html>

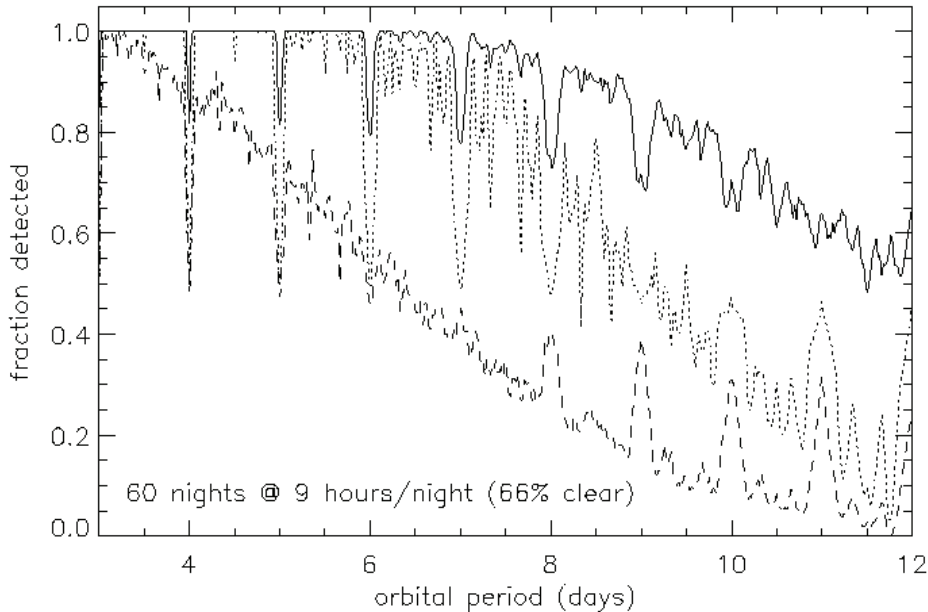


Fig. 2.— The fraction of transiting planet systems identified from three theoretical 2-month transit searches, where at least 3 distinct half-transits must be observed for the transit to be recovered. The simulated surveys are conducted with: a single telescope (dashed line); three telescopes in California (dotted); three telescopes in California, Arizona and the Canary Islands (solid). (Adapted from Charbonneau 2003.) The transatlantic survey is mostly complete, with the exception of transits missed due to the diurnal cycle (the dips at integer periods) and the long period transits for which the survey cannot observe the required number of transits in the given time. The single-site survey has a reduced recovery rate, except at integer periods. The relative completeness at short period shows the benefit of using telescopes widely dispersed in longitude.

get stars ($V \lesssim 13$), which facilitate critical followup observations of a detected transiting planet, such as measuring the stellar radial velocity variation or even direct studies of the planet. The Trans-atlantic Exoplanet Survey (TrES⁴) transit campaign builds upon the success of the STARE project, which identified the first transits from an exoplanet (Charbonneau et al. 2000). The survey is being conducted with a network of three planet-finding 10 cm telescopes: the original STARE telescope (now located in Tenerife, P.I.: T. Brown, NCAR), together with the PSST (Arizona, P.I.: E. Dunham, Lowell Observatory) and Sleuth (Palomar Observatory, P.I.: D. Charbonneau, Harvard). The wide longitudinal separation between sites is designed to maximize coverage of the selected field of stars (see Figure 2).

⁴<http://www.astro.caltech.edu/~ftod/tres/tres.html>

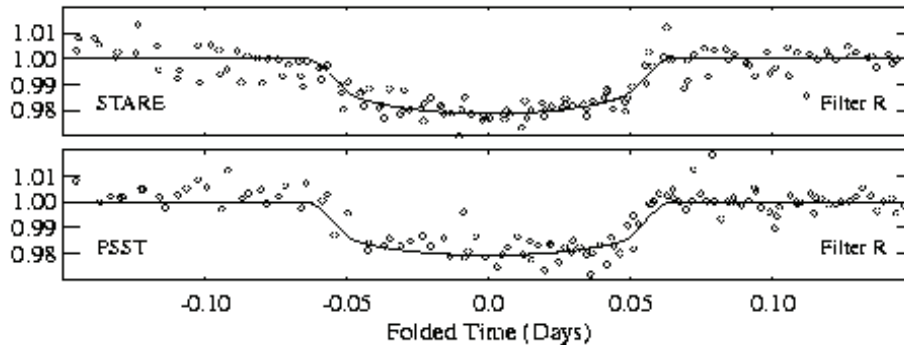


Fig. 3.— R filter time series photometry of TrES–1 obtained with PSST and STARE, overplotted with a theoretical light curve. (Adapted from Alonso et al. 2004.) The brightness of the star is reduced by 0.023 mag, corresponding to a $1.08 R_{\text{Jup}}$ object occulting a $0.85 R_{\odot}$ star.

Last year, the TrES collaboration discovered the planet TrES–1 (Alonso et al. 2004: see Figure 3), a Jupiter–sized planet with a mass of $0.75 M_{\text{Jup}}$ orbiting a K0V star every 3.03 days. At 150 pc away, TrES–1 is the closest planet discovered using the transit method. The masses and radii of the known transiting gas giants are shown in Figure 4, together with those of Saturn and Jupiter.

The radius of TrES–1 is more like those of the distant OGLE planets than that of the nearby HD 209458 b. It is clear that HD 209458 b and OGLE–TR–10 b display larger radii and lower densities than the other 5 planets, and this may indicate the presence of additional heating sources. One possible source is the presence of an unseen companion which would perturb HD 209458 b from its otherwise tidally circularized orbit. The tidal damping of this eccentricity would provide internal heating (Bodenheimer et al. 2001, 2003). Guillot & Showman proposed that the strong irradiation by the star of a hot Jupiter and the inhomogeneous atmosphere could store kinetic energy in the atmosphere and lead to a transfer of energy to the interior (Guillot & Showman 2002; Showman & Guillot 2002). However, Burrows et al. (2003) asserted that they can model HD 209458 b without an auxiliary heat source, assuming the planetary radius is at the lower end of the observed range. The future study of the new transiting hot Jupiters that TrES will discover will hopefully help us clarify the difference in the structure of these transiting planets.

The transit method for detecting extrasolar planets is a developing field, and upcoming satellite–based transit missions such as Kepler (Borucki et al. 2003) will look for other Earths. Further understanding of the parameter space explored by transit observations, and their observational biases and detection rates, will be required before we attempt the discovery of

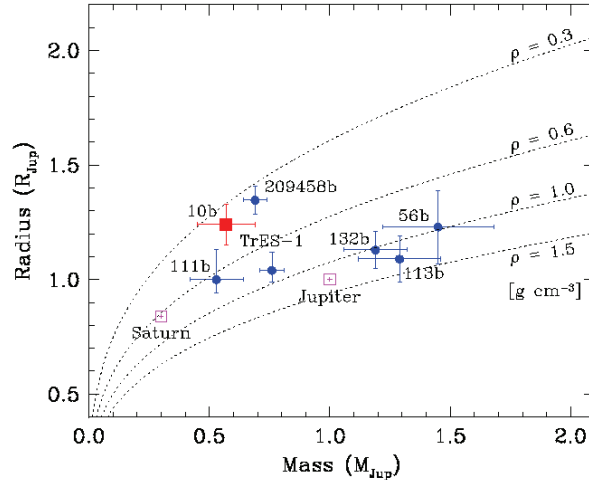


Fig. 4.— Radii of the currently known transiting planets plotted versus their masses, with two solar system gas giants for comparison. Lines of constant density are designated by dashed lines. The most recently discovered planet (OGLE–TR–10b) is identified by a square. (Figure from Konacki et al. 2004a.) Despite having a mass similar to TrES–1, HD 209458 b has a radius about 1.35 times that of the Jupiter–sized TrES–1, and is half as dense.

terrestrial–planets around solar–type stars.

2. Sleuth: Initial Observations and Data Analysis

A significant part of my thesis work and my contribution to the TrES survey is the operation of Sleuth⁵ (O’Donovan et al. 2004), our 10 cm TrES telescope which is located at Palomar Observatory. Sleuth has a f/2.8 lens that images a $6^\circ \times 6^\circ$ field of view onto a 2048×2048 back–illuminated CCD camera. The angular resolution is $10''/\text{pixel}$. The attached filter wheel contains SDSS g , r , i and z filters, and a Bessell R filter.

Each night, I run a script from Caltech for that night’s observing session. The automatic dome closure time is set, based on the current time for sunrise. The initial dome opening is performed by the 200” night assistant who will also override the nightly script and close the dome if weather threatens. Additional protection from inclement weather is provided by the 48” weather station. Upon dome opening, the script obtains calibration r –band evening sky flats. It determines when the target field has risen and then tracks the target star within

⁵<http://www.astro.caltech.edu/~ftod/tres/sleuth.html>

that field. The script continues to take r -band observations of the target field with a cadence of about 2 minutes until the field has set. Automatic focus adjustments are made when the temperature or the telescope filter changes. Morning r -band sky flats and darks are obtained just before the system is put to sleep and the data ftp’ed to Caltech. During dark time, I take multicolor (SDSS g , i & z) photometry, which I use to produce a master image and a master list of stars in the field.

I have developed scripts to automate the observations and data analysis. Only the monitoring of the quality of the raw images and data products is required. I calibrate the data automatically at Caltech and then perform image-subtraction photometry based on Alard (2000) to produce nightly time series. First, I view a sample of the night’s images to check for clouds or condensation. The median bias image and sky flat are created for that night. The bias image is subtracted from the raw images, which are then divided by the sky flat. A diagnostic plot of the average flux from the stars and sky background, together with the offset and rotation of each image, is produced for visual inspection. I reject images with abnormal stellar or sky fluxes – these are usually cloudy images or images taken during dome closure. A list of the position and magnitude of the stars in each of the remaining calibrated images is generated using aperture photometry. This list is matched with the master list to derive the transformation coefficients for spatially interpolating the image. The calibrated images are interpolated, and then a reference image is subtracted from each interpolated image. Again, I visually examine a sample of these subtracted images to verify that the subtraction residuals are low. Aperture photometry is then performed on the subtracted images.

Once we decide to change target fields (see §3), I collate the photometry from the current field to produce light curves for each star, such as the examples given in Figure 5, and examine these light curves for transit-like signals. First I assemble the aperture photometry from every night in order to produce a time series for each star in our field. These timeseries are organized in batches of 1000 stars. A histogram of each light curve is generated and the dispersion “ σ ” is estimated as the width (centered on the median of the data) which contains 95% of the data. Bad data points are identified as lying beyond 10σ and are culled. Data obtained with large field-of-view CCDs can suffer from systematic effects, such as those caused by changing photometric conditions or a variable point spread function (PSF). I therefore attempt to reduce these systematics by decorrelating each batch of stars: the least-squares fit to each light curve from a linear combination of the other light curves in the same batch is computed using singular value decomposition (SVD) and then subtracted from the individual light curve. However, these effects may vary across the detector, impeding removal from the data. We are investigating a new method to account for this (Tamuz et al. 2005). Finally, I average the decorrelated observations to 9 minute bins. This reduces the

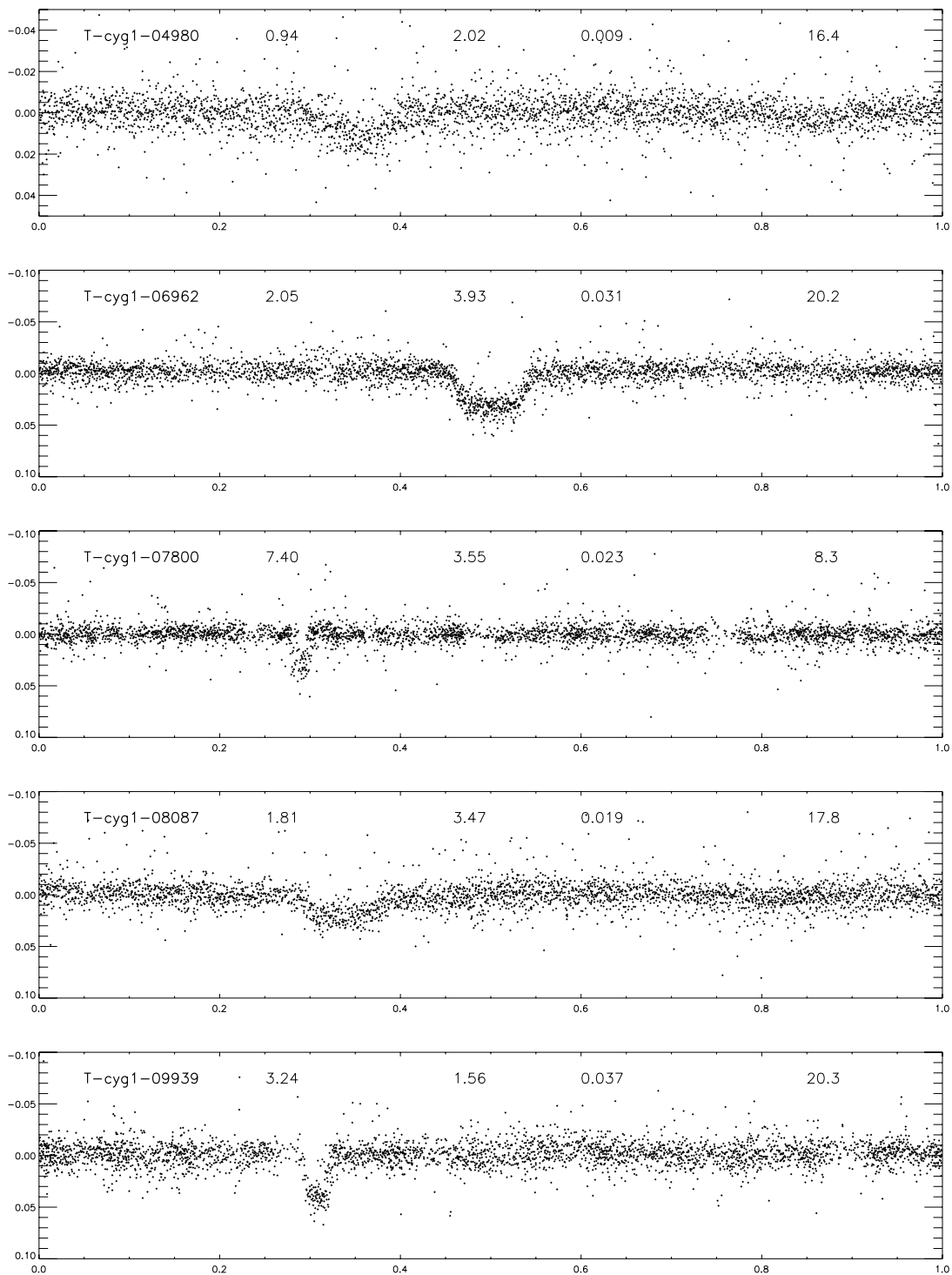


Fig. 5.— Sample time series photometry of several transit candidates from a field in Cygnus observed with Sleuth. From left to right, the name of the candidate and the period and depth of each transit are given, together with the Signal Detection Efficiency (SDE), a measure of the significance of the detection.

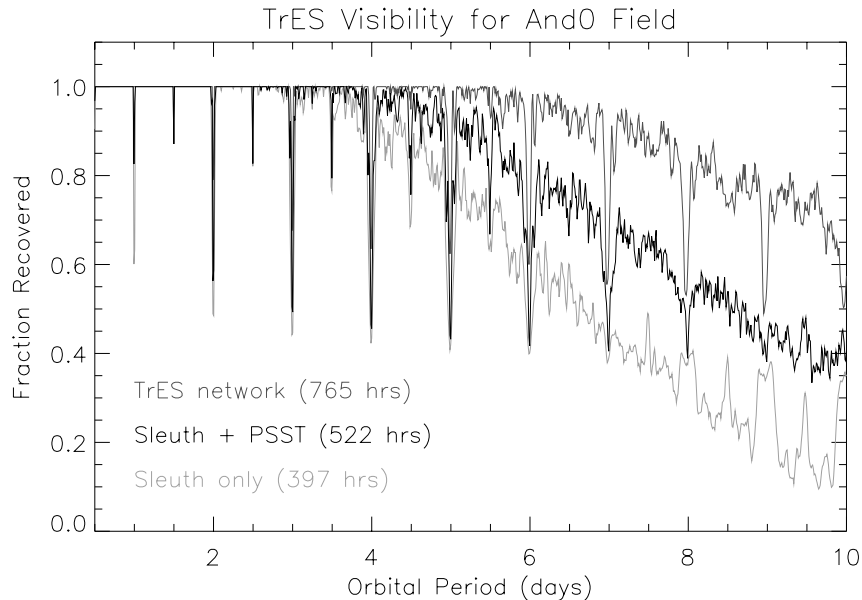


Fig. 6.— An example transit visibility plot for the Andromeda field derived from observations made using all three TrES telescopes. The fraction of transit signals with a given period that should be identifiable from the TrES data is plotted, assuming a requirement of observing 3 distinct transit events. Overplotted is the fraction identifiable from the Sleuth observations alone, and from the combined Sleuth/PSST data set. This shows the incremental coverage obtained by combining the data sets from the three telescopes.

amount of CPU time required for our transit search while maintaining a good time sampling of the ~ 3 hour duration of a transit.

3. Sleuth as Part of TrES

The TrES⁶ network adopts the following observing strategy for each target field that we select. The TrES telescopes observe our target field nightly as weather permits. Each group calibrates and analyzes data the following day, to the point of producing time series photometry. Every week, the effective transit visibility is calculated (see Figure 6). Eventually, the decision is made to cease observations and switch to a new field. The chosen “Field Honcho”⁷ concatenates the time series data from all three sites. The Field Honcho then

⁶<http://www.astro.caltech.edu/~ftod/tres/tres.html>

⁷I am Honcho for 5 of out 9 current TrES fields that Sleuth has observed.

performs a search of the time series using the box-fitting transit-search algorithm (TSA) of Kovács et al. (2002). He produces a list of candidates with periods ranging from 0.1 to 12 days from the output of the TSA. This algorithm assumes the simple two-step light curve of a flat transit, ignoring the effects of limb darkening. For a given light curve, it calculates a least-squares fit of the three parameters $\{\delta, q, t_0\}$ to the data for each trial period in the given range, where δ is the transit depth, q is the fractional transit length and t_0 is the epoch of the transit. The TSA then determines the “Signal Residue” (SR, a measure of the strength of the signal with that fit) for each period, and the best-fit period is that with the largest SR. The algorithm also characterizes the ability to detect each transit signal above the noise by the “Signal Detection Efficiency” (SDE), which is the difference between the peak and average SR values divided by the standard deviation of the SR.

Brown (2003) estimates the yield of a wide-field survey to be one transiting planet per 25,000 stars monitored, assuming a transit visibility function of 50% for periods less than 3 days. The TrES survey is now monitoring approximately 10,000 stars per field with sufficient photometric precision to detect a 1% transit⁸ (see Figure 7), and our transit visibility is close to 100% for periods less than 3 days. Therefore, the survey should produce a new transiting planet for almost every field observed. In order to find these planets, the Field Honcho must examine the list of candidates to identify and reject systems which are not true planetary systems but which produce transit-like light curves.

4. Confirmation and False Positive Rejection

Any wide-field transit survey will accumulate numerous candidate planets that turn out to be false detections, as there are several astronomical systems that can mimic the light curve of a transiting hot Jupiter. Brown (2003) examined the frequency of these false alarms for a typical wide-field, ground based survey. The three most common impostors involve eclipsing binary stars. Grazing incidence eclipsing binaries may produce the same flux reduction as a planetary system (I). The blending of the light from an edge-on binary system with that from a third star can also be mistaken for a transit. In this case, the third star may be bound to the binary system to form a triple system (II), or it may just be a foreground star (III). Brown (2003) found that for each transiting planet a TSA identifies, it will likely mistakenly identify 6 grazing incidence binaries and 6 blended eclipsing binaries

⁸We require $n = 3$ distinct transits, which typically last $t = 3$ hours, and we average our data to $b = 9$ minute bins. From Eqn. 1, the required precision is about 1.6% per measurement for a 5σ detection of the transit.

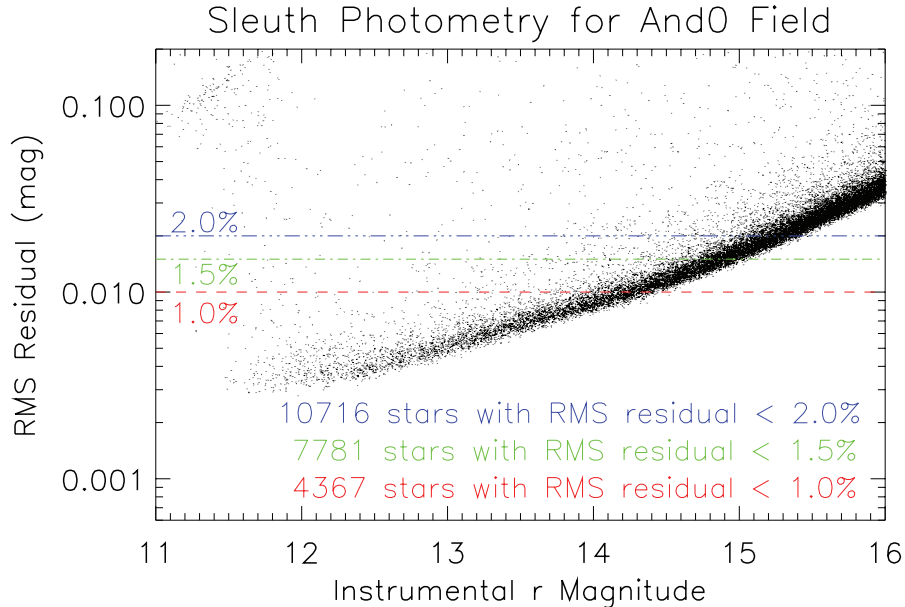


Fig. 7.— The calculated RMS versus instrumental r magnitude for the 26,000 brightest stars in our And0 field. The number of stars with RMS below 1%, 1.5% and 2% are shown.

as transits.

The first step in culling the list of potential candidates is to search publicly available star catalogs, such as Tycho-2 (Høg et al. 2000), 2MASS PSC⁹ (Cutri et al. 2003) and USNO-B (Monet et al. 2003), to obtain the proper motions and visible/infrared colors of the host stars, if available. A large proper motion of the host star suggest that the star is a nearby dwarf, rather than a distant giant star. (A 1% transit around such a star would indicate a stellar companion, and a short period would position the “companion” within the radius of the primary.) However, a negligible proper motion does not necessarily imply that the star is a giant. An image of the sky surrounding each candidate can be obtained from the online Digitized Sky Survey (DSS¹⁰) to identify nearby stars which may be blended in the fields of view of small-aperture telescopes. Finally, Brown’s $J - K$ color test can be applied: our target stars are main-sequence stars with radii $R_* \lesssim 1.3R_\odot$ around which a Jupiter-sized planet would have a transit depth $\delta \gtrsim 0.01$, and the $J - K$ color of such stars ranges from 0.25 to 1.0; however, a $J - K$ color in excess of 0.5 implies the star is

⁹The search tool for the All-Sky Point Source Catalog is available at <http://irsa.ipac.caltech.edu/applications/Gator/>.

¹⁰<http://archive.stsci.edu/dss/>

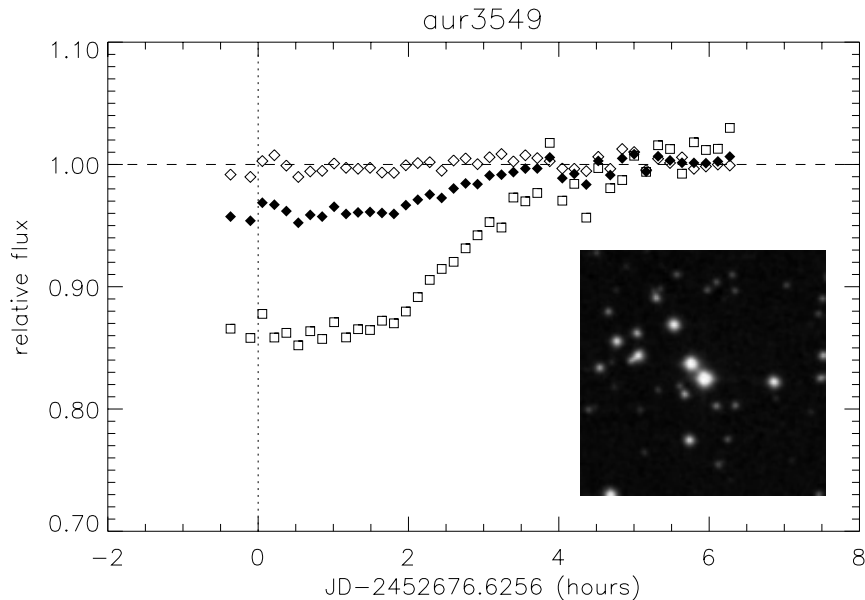


Fig. 8.— An example of the use of higher angular resolution to identify blended systems. (From Charbonneau et al. 2004.) This star was identified as a transit candidate based on the $\sim 1\%$ transit-like PSST photometry (black diamonds). When higher angular resolution photometry from a 14-inch telescope is examined, we can see the constant light curve of the central source (open diamonds) and the eclipsing nature of the fainter star (open squares). The true depth is $\sim 14\%$, clearly a stellar eclipse rather than a planetary occultation. The inset figure is a $2' \times 2'$ DSS image of the candidate star 3549 in Auriga. The two stars at the center are unresolved in the PSST photometry.

probably a giant, whereas the stars with $J - K$ less than 0.35 are mostly dwarfs (Brown 2003). Note that as the target stars are nearby dwarfs and this is an infrared color test, the effect of interstellar reddening can be ignored. For a typical system $d \sim 100$ pc away, the interstellar extinction in the V -band is given by: $A_V \sim 1.6(d/\text{kpc}) \text{ mag} \sim 0.16 \text{ mag}$ (Binney & Merrifield 1998, Eqn. 3.66). And so the effect of reddening on the $J - K$ color is $A_J - A_K = (0.282A_V - 0.114A_V) \sim 0.03 \text{ mag}$, using the extinction conversion factors derived by Cardelli et al. (1989).

Further observations are then necessary, both spectroscopic and photometric. With rapid, multicolor and high angular resolution photometry, it may be possible to resolve blended systems (see Figure 8) or to identify grazing eclipsing binaries by their V-shaped light curves. A color-dependent transit light curve may also be observed, indicative of a binary where the component stellar colors are different. The stellar companions in eclipsing binaries induce radial velocities greater than 1 km/s in the primaries. Medium resolution

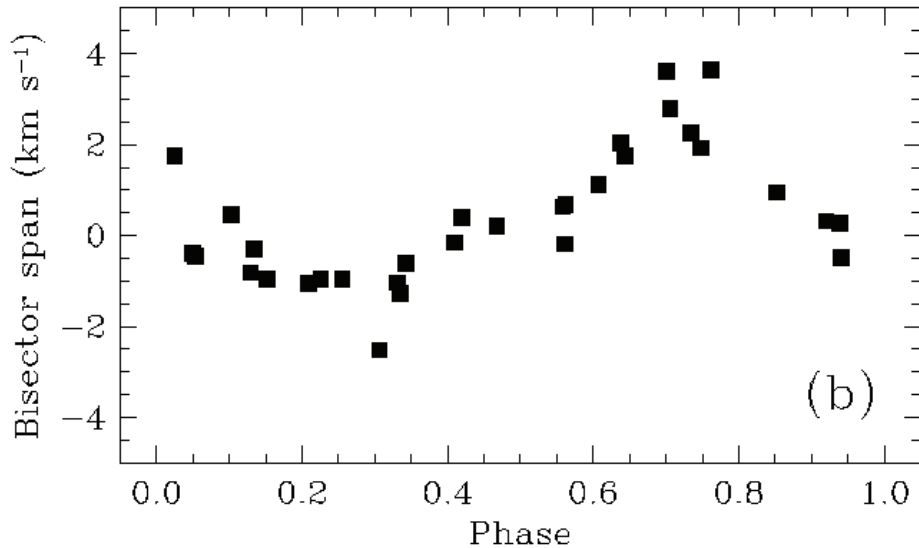


Fig. 9.— Bisector span measurements from the spectra of GSC 01944–02289. (Taken from Mandushev et al. 2005.) There is an obvious variation as a function of phase, which indicates contamination by the light from a third star.

spectroscopy would eliminate such candidates, and also provide spectral information such as the spectral type, effective temperature and surface gravity of the host star.

The difficulty of rigorously discarding all the eclipsing binaries from a list of candidates is highlighted by the recent case of GSC 01944–02289 (Mandushev et al. 2005). Detected as part of the TrES survey, and originally thought to be a transiting brown dwarf, detailed examination of the spectra of the system revealed it to be a hierarchical triple system. The nature of the primary F star led to this confusion: the light from the primary (89% of the total) overwhelmed that from the eclipsing binary, and the spectral lines of the primary were broadened by its rapid rotation ($v \sin i \sim 34\text{km/s}$). The slight difference in effective temperature between the F primary and one of the components of the binary (a G star) also reduced the color–dependence of the system’s light curve. In spite of this insidious blend, Mandushev et al. (2005) were able to identify the true nature of GSC 01944–02289 through a bisector¹¹ analysis of the spectral line shapes. The velocities corresponding to the top and bottom of the line bisectors of spectral features were computed and the difference between these values (the bisector span: Torres et al. 2004a) was plotted as a function of phase (see Figure 9).

¹¹The bisector of a spectral line is the locus of points midway between the red and blue wings of the spectral feature.

Despite the numerous false positive detections inherent in such a campaign, the TrES survey was able to identify one real transiting planet, TrES-1 (Alonso et al. 2004), by the application of these techniques to winnow out the eclipsing binary systems. The success of these procedures and their continued development are important for current planet-finding surveys and critical for future satellite missions. The planned space surveys will identify candidate planets beyond the reach of current high-resolution spectroscopy and will require new methods of false positive rejection.

5. TrES Followup Observations

Once the Field Honcho has assembled a list of candidates, he organizes the followup observations required to confirm the true nature of the candidate planets. The Honcho collects data from the 2MASS, USNO-B, Tycho-2 and DSS catalogs to determine the likelihood that each candidate is a nearby, single FV-MV star.

If required, I setup followup multicolor photometry with Sherlock¹² (Kotredes et al. 2004). Sherlock has a larger aperture (25 cm), a longer focal ratio (f/6.3) and a higher angular resolution (1.7"/pixel) than Sleuth, and resides in the same enclosure at Palomar Observatory. The 30' × 30' field of view of the telescope is imaged onto a 1024 × 1024 CCD. Three non-standard color interference filters are installed, labeled "blue", "green" and "red". The narrowness of these filters, together with their sharp cuton and cutoff, reduces color-dependent effects. This makes them suitable for observing the color-dependence of the light curve of a candidate transiting planet. In order to perform observations with Sherlock, I create a list of candidate planets based on the results from the various TrES survey fields. Each night, I determine which candidates are predicted to transit, and select from these the candidate with the optimal observing conditions. Using an automated script similar to that used for Sleuth, I then obtain observations of this candidate throughout the night, together with calibration darks and sky flats, and ftp the data back to Caltech. The bias is subtracted from the images, which are then divided by the flats. I perform aperture photometry on the calibrated images to produce a nightly time series for the target star. I am still in the process of automating these procedures as I have done for Sleuth.

Concurrent with my multicolor photometry, collaborator Dr. D. Latham (CfA) performs multiepoch spectroscopy (with $R \sim 30,000$ and errors of about 0.4 km/s) using the Digital Speedometers (Latham 1992). Candidates that are observed to have radial velocities consistent with stellar companions are rejected. Candidates for which we have no evidence of a

¹²<http://www.astro.caltech.edu/~ftod/tres/sherlock.html>

stellar nature are observed with Keck/HIRES (with $R \sim 65,000$ and errors of about 10–15 m/s) to search for the radial velocity orbit induced by a planetary mass object. HIRES spectra are also examined for evidence of blended impostor systems following Torres et al. (2004b).

As the discovery team of TrES-1, we have obtained Director’s Discretionary time to perform detailed studies of this nearby transiting planet using space-borne telescopes. The precision of these observations of bright stars approaches the photon-noise limit. Our observations of TrES-1 using the IRAC camera on Spitzer (Charbonneau et al. 2005) were timed to coincide with the secondary eclipse so as to allow a direct detection of emission from the planetary atmosphere. We have performed eclipse timing to measure the orbital eccentricity of the planet. We have an upcoming observation with the HST to improve our estimates for the radius and inclination of the planet from observations with ACS/HRC. Observations with NICMOS may enable us to study water vapor absorption in the atmosphere and place constraints on the composition and structure of the upper atmosphere.

6. Telescope Facility Usage

I plan to use Sherlock as a primary means of obtaining multicolor, higher angular resolution photometry of promising candidates. However, Sherlock is an experimental system built of commercial components, and is not yet operating with sufficient reliability. I will use the 60-inch to gather high-precision multi-color time-series photometry of candidates for which low-resolution spectroscopy has revealed no significant Doppler variations. I will select two candidates per month, and observe each star for 6 hours spanning the predicted time of transit.

High resolution spectroscopic observations (beyond the capabilities of the Palomar 200-inch) of our candidate planets are a necessary part of our followup strategy. Although such observations could be gathered through collaborations with G. W. Marcy (Keck/HIRES) and W. D. Cochran (HET/HRS: Cochran et al. 2004), we intend to propose for Caltech Keck/HIRES time directly, to observe candidates that have survived our photometric and spectroscopic followups. A planet with a mass as low as $0.2M_J$ around a $V = 12$ star (typical of the TrES targets) can be detected with 4σ confidence from a 35 minute integration¹³ with HIRES. We will propose to observe the target stars several times a night for approximately 3 nights to obtain radial velocity estimates at significantly difference orbital phases.

¹³Calculated using the formula given in Charbonneau (2003).

7. Principal Goals of Thesis Work as Part of the TrES Campaign

As the main observer on Sleuth and a member of the TrES consortium, I will be directly involved in the discovery of new transiting hot Jupiters and obtaining high-precision values for the masses and radii of these planets. By deriving their average densities and surface gravities, and by learning how the radius of a Jupiter-like planet varies with the orbital properties, and the stellar type and environment, I may begin to provide constraints of the current models for strongly irradiated gas giants. By searching for anomalous planetary radii similar to that of HD 209458 b, I can try to identify the cause of this over-inflation.

With larger facilities, numerous followup observations of each new TrES transiting planet will be possible (while similar observations of the fainter OGLE-III transiting systems are beyond current capabilities). With high-precision photometric observations, I will be able to further confine the planetary system parameters, as well as search for additional objects in the system. Spectroscopic observations of the eclipses will study the absorption and emission due to the planetary atmosphere.

Note on Supervision of Thesis

Prof. Charbonneau, now at Harvard, will continue to be my main advisor, while Prof. Hiltenbrand will provide local supervision and assist me in obtaining Caltech telescope time.

Ph.D. Timeline

For the remainder of my thesis work, I will continue to perform observations with Sleuth as part of the TrES survey, which will result in the detection of candidate transiting planets. Sleuth should observe 15–30 new fields in that time. I will conduct follow-up observations of the candidates with Sherlock as part of the false positive rejection procedure.

As Field Honcho, I will supervise the spectroscopic and photometric follow-up of candidates from 10 fields, and will prepare papers based on the results of these observations. A paper concerning our recent observations in the Andromeda field is in preparation.

I am participating in the Spitzer and HST observations of TrES-1, and will continue to be a part of the observing teams for such observations of newly discovered transiting planets. Beginning the fourth year of my thesis, once we have several transiting planets to observe, I plan to conduct my own detailed studies of the planets, with Keck and Spitzer.

This study of transiting planets should be mostly complete by Winter 2007, when I plan to begin writing my thesis. I would then defend in Spring 2007.

REFERENCES

- Alard C., 2000, *A&AS*, 144, 363
- Alonso R., Brown T. M., Torres G., et al., 2004, *ApJ*, 613, L153
- Bakos G. Á., Lázár J., Papp I., Sári P., Green E. M., 2002, *PASP*, 114, 974
- Binney J., Merrifield M., 1998, *Galactic Astronomy*. Princeton University Press, Princeton, NJ
- Bodenheimer P., Laughlin G., Lin D. N. C., 2003, *ApJ*, 592, 555
- Bodenheimer P., Lin D. N. C., Mardling R. A., 2001, *ApJ*, 548, 466
- Borucki W. J., Koch D. G., Lissauer J. J., et al., 2003, *Proceedings of SPIE*, 4854, 129
- Boss A. P., 1997, *Science*, 276, 1836
- Boss A. P., 2000, *ApJ*, 536, L101
- Boss A. P., 2001, *ApJ*, 563, 367
- Bouchy F., Pont F., Santos N. C., et al., 2004, *A&A*, 421, L13
- Brown T. M., 2003, *ApJ*, 593, L125
- Brown T. M., Charbonneau D., Gilliland R. L., Noyes R. W., Burrows A., 2001, *ApJ*, 552, 699
- Burrows A., Sudarsky D., Hubbard W. B., 2003, *ApJ*, 594, 545
- Cardelli J. A., Clayton G. C., Mathis J. S., 1989, *ApJ*, 345, 245
- Charbonneau D., 2003, *Space Science Reviews*, astro-ph/0302216
- Charbonneau D., Allen L. E., Megeath T., et al., 2005, to appear in *ApJ*
- Charbonneau D., Brown T. M., Dunham E. W., et al., 2004, *AIP Conf. Proc.*, 713, 151
- Charbonneau D., Brown T. M., Latham D. W., Mayor M., 2000, *ApJ*, 529, L45
- Charbonneau D., Brown T. M., Noyes R. W., Gilliland R. L., 2002, *ApJ*, 568, 377
- Cochran W. D., Endl M., McArthur B., et al., 2004, *ApJ*, 611, L133
- Cutri R. M., Skrutskie M. F., van Dyk S., et al., 2003, *VizieR Online Data Catalog*, 2246, 0

- Guillot T., Showman A. P., 2002, *A&A*, 385, 156
- Henry G. W., Marcy G. W., Butler R. P., Vogt S. S., 2000, *ApJ*, 529, L41
- Høg E., Fabricius C., Makarov V. V., et al., 2000, *A&A*, 355, L27
- Horne K., 2003, *ASP Conf. Ser.*, 294, 361
- Konacki M., Torres G., Jha S., Sasselov D. D., 2003, *Nat*, 421, 507
- Konacki M., Torres G., Sasselov D. D., Jha S., 2004a, accepted to *ApJ*, astro-ph/0412400
- Konacki M., Torres G., Sasselov D. D., et al., 2004b, *ApJ*, 609, L37
- Kotredes L., Charbonneau D., Looper D. L., O'Donovan F. T., 2004, *AIP Conf. Proc.*, 713, 173
- Kovács G., Zucker S., Mazeh T., 2002, *A&A*, 391, 369
- Latham D. W., 1992, *ASP Conf. Ser.*, 32, 110
- Laughlin G., Wolf A., Vanmunster T., et al., 2005, *ApJ*, in press
- Mallén-Ornelas G., Seager S., Yee H. K. C., et al., 2003, *ApJ*, 582, 1123
- Mandushev G., Torres G., Latham D. W., et al., 2005, *ApJ*, 621
- Mayor M., Queloz D., 1995, *Nat*, 378, 355
- Mazeh T., Naef D., Torres G., et al., 2000, *ApJ*, 532, L55
- Monet D. G., Levine S. E., Canzian B., et al., 2003, *AJ*, 125, 984
- O'Donovan F. T., Charbonneau D., Kotredes L., 2004, *AIP Conf. Proc.*, 713, 169
- Pollack J. B., 1984, *ARA&A*, 22, 389
- Pollack J. B., Hubickyj O., Bodenheimer P., et al., 1996, *Icarus*, 124, 62
- Pont F., Bouchy F., Queloz D., et al., 2004, *A&A*, 426, L15
- Showman A. P., Guillot T., 2002, *A&A*, 385, 166
- Struve O., 1952, *Observatory*, 72, 199
- Tamuz O., Mazeh T., Zucker S., 2005, *MNRAS*, 356, 1466
- Torres G., Konacki M., Sasselov D. D., Jha S., 2004a, *ApJ*, 609, 1071
- Torres G., Konacki M., Sasselov D. D., Jha S., 2004b, *ApJ*, 614, 979
- Udalski A., Paczynski B., Zebrun K., et al., 2002a, *Acta Astron.*, 52, 1

Udalski A., Pietrzynski G., Szymanski M., et al., 2003, *Acta Astron.*, 53, 133

Udalski A., Szewczyk O., Zebrun K., et al., 2002b, *Acta Astron.*, 52, 317

Udalski A., Zebrun K., Szymanski M., et al., 2002c, *Acta Astron.*, 52, 115

Vidal-Madjar A., Lecavelier des Etangs A., Désert J.-M., et al., 2003, *Nat*, 422, 143